Am J Nucl Med Mol Imaging 2017;7(3):84-91
www.ajnmmi.us /ISSN:2160-8407/ajnmmi0049356

Original Article

Correlation between two methods of florbetapir PET quantitative analysis

Christopher Breault[1,2], Jonathan Piper[3], Abhinay D Joshi[1], Sara D Pirozzi[3], Aaron S Nelson[3], Ming Lu[1], Michael J Pontecorvo[1], Mark A Mintun[1], Michael D Devous[1]

[1]Avid Radiopharmaceuticals (A Wholly Owned Subsidiary of Eli Lilly and Company), 3711 Market St, Philadelphia 19104, PA, U S A; [2]Spectrum Dynamics Medical Inc. (A Biosensors International Group Company), 2478 Embarcadero Way, Palo Alto 94303, CA, U S A; [3]MIM Software Inc., 25800 Science Park Drive, Suite 180, Cleveland 44122, OH, U S A

Received January 20, 2017; Accepted May 10, 2017; Epub July 15, 2017; Published July 30, 2017

Abstract: This study evaluated performance of a commercially available standardized software program for calculation of florbetapir PET standard uptake value ratios (SUVr) in comparison with an established research method. Florbetapir PET images for 183 subjects clinically diagnosed as cognitively normal (CN), mild cognitive impairment (MCI) or probable Alzheimer's disease (AD) (45 AD, 60 MCI, and 78 CN) were evaluated using two software processing algorithms. The research method uses a single florbetapir PET template generated by averaging both amyloid positive and amyloid negative registered brains together. The commercial software simultaneously optimizes the registration between the florbetapir PET images and three templates: amyloid negative, amyloid positive, and an average. Cortical average SUVr values were calculated across six predefined anatomic regions with respect to the whole cerebellum reference region. SUVr values were well correlated between the two methods (r^2 = 0.98). The relationship between the methods computed from the regression analysis is: Commercial method SUVr = (0.9757*Research SUVr) + 0.0299. A previously defined cutoff SUVr of 1.1 for distinguishing amyloid positivity by the research method corresponded to 1.1 (95% CI = 1.098, 1.11) for the commercial method. This study suggests that the commercial method is comparable to the published research method of SUVr analysis for florbetapir PET images, thus facilitating the potential use of standardized quantitative approaches to PET amyloid imaging.

Keywords: Amyloid imaging, amyloid PET, PET quantitation, florbetapir, amyvid

Introduction

Imaging biomarkers that bind to aggregated Aβ peptides in amyloid plaques have the potential as a diagnostic aid in the evaluation of patients with cognitive impairment by providing information regarding presence or absence of relevant neuropathology [1]. The introduction of the PET ligand Pittsburgh compound B (^{11}C-PiB) in 2004 [2], has helped pave the way for the development of several ^{18}F labeled compounds including florbetaben ^{18}F [3], flutemetamol ^{18}F [4], and florbetapir ^{18}F [5].

In a research setting, the quantification of these various amyloid tracers has involved the use of non-standardized tools or software. For example, Avid Radiopharmaceuticals developed a method that has been widely used in clinical trials [5, 6, 9-12], is highly correlated with freesurfer/MRI based methods [13], and has been validated by comparison to autopsy results [14, 15]. As previously described [8] the research method consists of a semi-automated analysis utilizing SPM2 [16] to align florbetapir PET images to standard Montreal Neurological Institute (MNI) [17] space using a florbetapir-specific template. Once aligned in standard space, pre-defined cortical regions of interest are applied to the image and used to calculate a Standard Uptake Value ratio, or SUVr value, using the whole cerebellum as a reference region.

The use of software that was intended for research requires some image-processing expertise and can require manual intervention, which limits its applicability for broader clinical use.

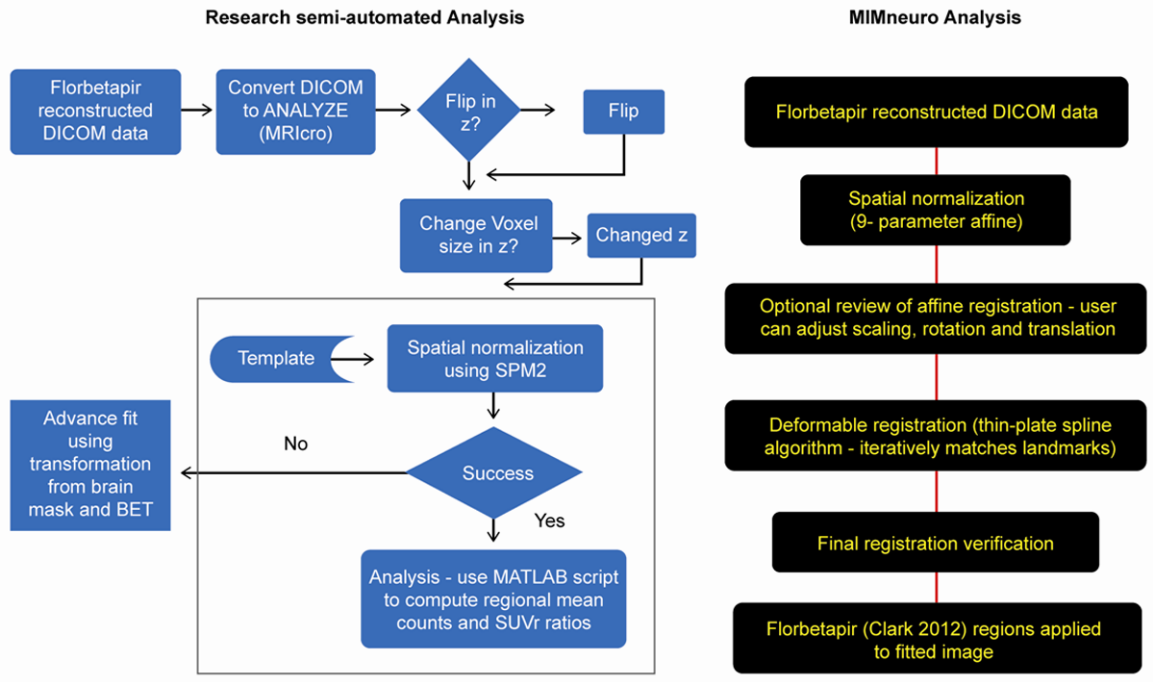

Figure 1. Diagrammatic representations of image processing steps using the research method and commercially available software.

Conversely MIMneuro, commercially available software, provides an alternative semi-automated florbetapir analysis method. MIM has developed a multi-template registration technique to align florbetapir PET images in standard space and apply regions of interest utilized in the research method [8, 15] to estimate SUVr.

Although the approved method for clinical interpretation of florbetapir PET scans consists of conducting a binary visual read for the detection of amyloid deposits, quantitation has proven useful as an adjunct to visual read for a number of other tracers in different applications [18-21]. The purpose of this paper is to validate the commercially available tool, MIMneuro, against a research method for SUVr calculation that was previously used in a large cross-sectional/longitudinal study [9, 10] and validated against autopsy evaluation [14, 15].

Materials and methods

This study employed a retrospective sample of all subjects with a valid florbetapir PET image (183 total) from a previously reported study [9] consisting of 78 images from subjects clinically diagnosed as cognitively normal (CN), 60 as mild cognitive impairment (MCI), and 45 as probable Alzheimer's disease (AD). The parent study was approved by appropriate institutional review boards and all subjects gave informed consent prior to performance of study procedures.

As described previously, all participants received a single administration of approximately 370 MBq (10 mCi) Florbetapir ^{18}F, followed approximately 50 minutes later by a 10-minute PET acquisition (2 × 5 minute frames). Images were reconstructed using an ordered subset estimation algorithm (4 iterations, 16 subsets, with a post-reconstruction Gaussian filter of 5 mm), and corrected for scatter and attenuation using commercial software packages for the respective scanners (Siemens: ECAT HR+PET and 16-slice Biograph PET/CT, GE: Discovery LS PET/CT and Advance PET/CT). No partial volume correction was performed. Each image was analyzed twice, once using the research method and once using the commercial method without intervention, to register florbetapir PET images into a template space where the regions of interest were applied to compute mean regional tracer uptake. For each method a cortical average SUVr was calculated as the average of six target regions relative to the cerebellum.

Research method for registration and SUVr calculation

For the research method [8], images were spatially normalized to a florbetapir PET template using a semi-automated algorithm in SPM 2. This method makes use of a non-linear registration algorithm [16] to register florbetapir PET images to a florbetapir PET template in MNI atlas space. The research method utilized a single florbetapir PET template generated by averaging both amyloid positive and amyloid negative registered brains, developed using the data acquired in a previous study [5]. An initial registration was applied to all the data and was referred to as fit 1. The non-linear registration results were visually checked for alignment of the patient brain to the template brain. Additional fitting steps involving the application of a brain mask and application of skull stripping, fit 2 and fit 3 respectively, could be applied in order to optimize image registration to the template (**Figure 1**), but were not employed for the primary analysis reported below.

A MATLAB script applied predefined anatomically relevant standard atlas space volumes of interest (VOIs) to calculate SUVr. The un-weighted cortical average SUVr values were calculated for relevant cortical regions: medial orbital frontal, lateral temporal, parietal, anterior cingulate, posterior cingulate, and precuneus, with the whole cerebellum used as a reference region. Derivation of the regions, rationale for choice of the reference region and agreement with histopathology has been described elsewhere [8, 15].

Commercial method for registration and SUVr calculation

MIMneuro 6.0.5 simultaneously optimizes the registration between the florbetapir PET image and three templates: amyloid negative, amyloid positive, and an average of the two. Each florbetapir-PET image from the analysis cohort was registered to template space using the multi-template registration to perform region-based SUVr calculation using atlas VOIs (**Figure 1**).

Eleven AD and 15 CN subjects with florbetapir-PET images [5] were used to create the florbetapir registration templates in MIM with a technique reported previously [22]. Each of the 26 subjects was registered to the same FDG-PET registration template included in the software. The images visually read as amyloid positive were count normalized to the whole cerebellum and averaged together to create an amyloid "positive" template. The images visually read as amyloid "negative" were similarly processed and averaged to create an amyloid negative template. The two average images were then averaged together to create a third, "average", template.

The simultaneous multi-template registration of florbetapir PET images occurred in a two-step process similar to the method reported previously [22] but modified to accommodate simultaneous multiple template optimization. First, a 9-parameter affine registration was used to determine an alignment into template space by maximizing the average normalized mutual information of the affine-transformed image to each of the three ("positive", "negative", "average") florbetapir-PET templates. This affine registration was then used to initialize an iterative process of landmark matching and thin-plate spline landmark-based deformation. Several hundred landmarks, located throughout the brain, particularly at tissue interfaces such as gray matter/CSF, were searched during each iteration. Similar to the affine registration, corresponding landmarks are chosen by optimizing image similarity metrics local to each landmark against all three templates simultaneously. The method of using all three templates simultaneously for registration optimization was developed to ensure that a variety of local florbetapir-PET uptake patterns are represented while minimizing systematic registration bias to the quantitative analysis. This registration bias is likely to occur if registering images to different templates based on similarity to each template individually.

The research VOIs used for SUVr calculation (medial orbital frontal, lateral temporal, parietal, anterior cingulate, posterior cingulate, precuneus, whole cerebellum) were transferred into MIMneuro florbetapir template space using the multi-template registration process described above for the research method's template image. Each voxel in template space (2 × 2 × 2 mm) was determined to be either included or excluded from the region based on determining the mapping from the center of that voxel in MIM florbetapir-PET template space to the corresponding position in MNI template space as

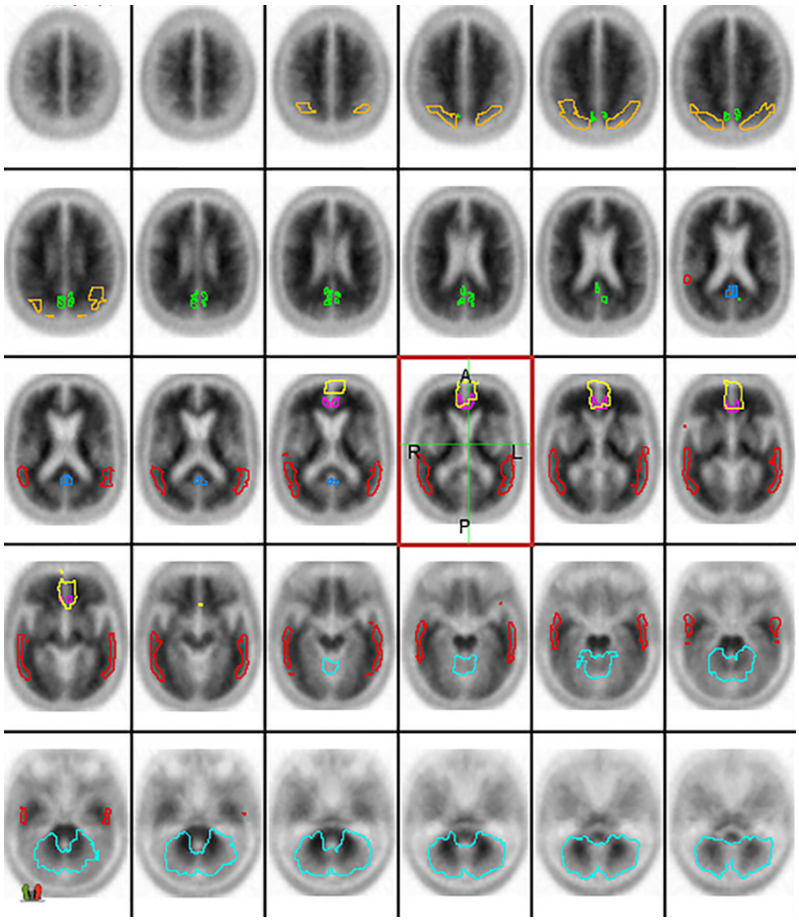

Figure 2. The global SUVr used for evaluation of amyloid uptake is composed of the average of six regions: medial orbital frontal (yellow), lateral temporal (red), posterior cingulate (blue), anterior cingulate (pink), lateral parietal (gold), and precuneus (green) relative to whole cerebellum (light blue) as shown here. The SUVr for this subject was 1.36 using the research semi-automated (SPM2) method and 1.35 using MIMneuro.

defined by the deformable transformation. Average SUVr was then computed as the mean of the mean voxel values within each atlas VOI in template space normalized to the mean voxel value of the cerebellum (**Figure 2**).

Statistical methods

Correlations between MIMneuro and the research method of florbetapir SUVr measurements were assessed using Pearson product-moment correlation analysis. With MIMneuro SUVr as a dependent variable and research SUVr as an independent variable, a linear regression function was fit and the regression parameters (intercept and slope) were estimated using a least squares method. The derived regression equation (MIMneuro SUVr = slope* research SUVr + intercept) was used to predict corresponding MIMneuro SUVr value for the research SUVr cutoff thresholds (SUVr = 1.1). The 95% confidence interval for this predicted value was calculated. Cook's Distance [23] was used to examine potential outliers. Observations with calculated Cook's D greater than 4/n (where n is the number observations in total) were considered as outliers [24].

Results

In this sample, individual scans were fit into template space without user intervention. The calculated SUVr using the research method ranged between 0.86 and 1.94, and between 0.83 and 1.84 using MIMneuro. A typical result demonstrating the overlays of the six cortical VOIs and cerebellar reference region is shown in **Figure 2**. The mean (SD) cortical SUVr for all 183 subjects with the research method was 1.19 (0.27) and 1.19 (0.26) for MIMneuro (**Table 1**). There were no between-method differences in SUVr within any of the individual diagnostic categories; AD-1.40 (0.27) versus 1.40 (0.25), MCI-1.05 (0.16) versus 1.05 (0.16), and CN-1.20 (0.28) versus 1.20 (0.27). The overall correlation between the two methods was 0.99, accounting for 98% of the variance. In addition to being well-correlated overall, the two methods were also well correlated on a regional basis (**Table 2**). The regional correlations ranged between 0.92 and 0.98 with the lowest correlations being obtained in the parietal region.

The slope of the regression line comparing the two quantitation methods approached 1.0 and the intercept approached 0 (**Figure 3**: MIMneuro_SUVr = 0.9757*research SUVr + 0.0299). Using the research method, the threshold for amyloid positivity has been previously

Table 1. Mean (Standard Deviation) SUVr for individual and composite cortical regions across diagnostic groups and for All subjects

	AD (n = 45)		MCI (n = 60)		CN (n = 78)		All Subjects (n = 183)	
Region of Interest	MIM[a]	Research[b]	MIM	Research	MIM	Research	MIM	Research
Anterior Cingulate	1.51 (0.32)	1.54 (0.37)	1.27 (0.31)	1.28 (0.32)	1.10 (0.19)	1.12 (0.24)	1.25 (0.31)	1.28 (0.34)
Frontal	1.30 (0.27)	1.28 (0.30)	1.10 (0.26)	1.11 (0.28)	0.97 (0.16)	0.96 (0.18)	1.09 (0.26)	1.09 (0.28)
Temporal	1.42 (0.28)	1.43 (0.29)	1.22 (0.28)	1.24 (0.29)	1.09 (0.17)	1.11 (0.22)	1.21 (0.27)	1.23 (0.29)
Posterior Cingulate	1.39 (0.24)	1.47 (0.31)	1.20 (0.26)	1.22 (0.28)	1.04 (0.16)	1.07 (0.17)	1.18 (0.26)	1.22 (0.29)
Precuneus	1.53 (0.29)	1.56 (0.33)	1.30 (0.32)	1.31 (0.32)	1.12 (0.20)	1.14 (0.22)	1.28 (0.31)	1.30 (0.33)
Parietal	1.28 (0.23)	1.24 (0.25)	1.14 (0.25)	1.11 (0.29)	1.00 (0.15)	0.95 (0.17)	1.11 (0.23)	1.07 (0.26)
Mean Cortical	1.40 (0.25)	1.40 (0.27)	1.20 (0.27)	1.20 (0.28)	1.05 (0.16)	1.05 (0.16)	1.19 (0.26)	1.19 (0.27)

Abbreviations: AD = Alzheimer's disease, CN = cognitively normal controls, MCI = mild cognitive impairment, SUVr = Standard Uptake Value Ratios. [a]MIMneuro, commercially available software; [b]Avid Radiopharmaceuticals research method, current standard in clinical trials and validated by comparison to autopsy results.

Table 2. Pearson product-moment correlation (r) across regions

	Anterior Cingulate	Frontal	Temporal	Posterior Cingulate	Precuneus	Parietal	Mean Cortical
All Subjects[a]	0.93	0.95	0.93	0.93	0.95	0.89	0.99

[a]All subjects (N = 183): Alzheimer's disease (n = 45), mild cognitive impairment (n = 60), cognitively normal (n = 68).

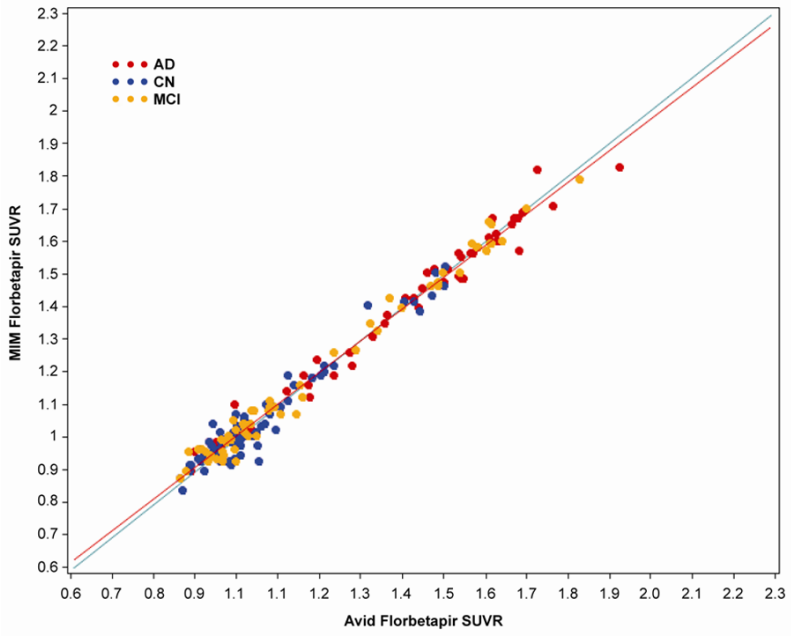

Figure 3. Scatter plot for the six region composite cortical SUVr for 183 subjects demonstrating the relationship between the research and commercially available methods. Abbreviations AD = probable Alzheimer's disease, CN = cognitively normal controls, MCI = mild cognitive impairment, SUVr = standard uptake value ratios.

reported as 1.10 [8, 15]. When research SUVr = 1.10, the MIMneuro SUVr (95% CI) = 1.10 (1.098, 1.11). Using the threshold of 1.10, 182 of 183 subjects were classified the same across the two software systems. One MCI subject's mean cortical SUVr was 1.08 with the research method and 1.11 using MIMneuro.

Of the 183 cases examined, 8 subjects were identified as outliers by calculation of Cook's distance. Each of these cases was reviewed to assess their overall fit to the template and in 7/8 cases benefited from the application of additional fitting steps (fit 2 and fit 3) using the research method. Overall correlation between the two methods improved from 0.9899 to 0.9920.

Discussion

In this study, we have shown that the two methods of SUVr analysis are well correlated across a range of subjects. Two different approaches of template registration methods provided consistent results in all three subject diagnostic groups with a correlation of 0.99 overall.

This research method had previously been validated against an autopsy cohort, 46 of whom had autopsy within one year of their florbetapir scan [8, 15]. Within this cohort, all 28 subjects

that had a neuropathological classification of moderate or frequent plaques by CERAD criteria had an SUVr > 1.10 whereas all 18 subjects with no or sparse plaques had an SUVr ≤ 1.10. The present study shows a slope of 1.0, correlation coefficient of 0.99 and a regression derived threshold of the MIMneuro SUVr equivalent of 1.10. This strategy of using a regression slope and derived threshold to compare analytic methods is similar to that employed in other studies with amyloid tracers [13, 25].

Although the present work focused on a single standard fit to template, additional image processing, including brain mask application and skull stripping, has been required in some previous instances using the research method [15]. In the present study, seven of the eight cases that were furthest from the line of identity benefitted from additional intervention and image processing, using the research method. Deformable registration applied within the MIMneuro software may increase the robustness of registration and reduce the need for further manual intervention. The MIMneuro software does include an option for manual adjustment of either the image registration or ROI placement. However these were not tested in the present study. Adjustment of the template registration has the ability to either improve or worsen the performance of the registration and thus requires additional training and expertise to recognize when the adjustment has optimized the fit to the template space. Thus, additional studies will be required to determine the performance of the MIMneuro software in difficult cases, including those with advanced disease, atrophy, significant comorbid degenerative conditions, or poor placement in scanner that may require manual intervention to optimize registration.

A limitation of this work is that the test scans were collected in a research setting. However, the population reflects a clinically relevant sample of subjects. The MCI subjects in particular were either seeking diagnosis at the time of enrollment or had been diagnosed within the previous year.

Although quantitative analyses cannot substitute for expert image interpretation, it has been suggested that image quantitation could be helpful in assisting visual interpretation of amyloid PET [26-29]. Quantitative approaches are commonly used to aid in interpretation of other nuclear medicine imaging studies including PET [18-21], and quantitative analyses have been used to characterize the relationships between amyloid tracer binding and cognitive performance other biomarkers [6, 7, 30, 31]. The present demonstration that commercially available software packages can achieve similar results as the established research methods for quantitation of amyloid PET raise the possibility that quantitative estimates of tracer uptake/amyloid binding could be integrated into an algorithm for interpretation of scans in a clinical setting.

In summary, the two methods are well correlated across the entire SUVr range. The slope of the regression line converting the research method results to the commercial method results approaches 1 and the intercept approaches 0. The SUVr level defining an amyloid positive PET scan using both methods is 1.10 by both methods. Using the previously validated research method as a benchmark, these results suggest it is possible to achieve comparable quantitative information with software requiring less technical expertise and that the commercial method is comparable to the published research method of SUVr analysis for florbetapir PET images.

Compliance with ethical standards

Ethical Approval: No new human subjects were studied in this report. The analyses described here were performed on data from a previous study [8], which was performed in accordance with the ethical standards of the institutional and/or national research committee and with the 1964 Helsinki declaration and its later amendments or comparable ethical standards.

Disclosure of conflict of interest

None.

Address correspondence to: Dr. Aaron Nelson, MIM Software Inc., 25800 Science Park Drive, Suite 180, Cleveland 44122, OH, U S A. Tel: 215-298-0700; Fax: 216-455-0601; E-mail: asnelson@mimsoftware.com

References

[1] Johnson KA, Minoshima S, Bohnen NI, Donohoe KJ, Foster NL, Herscovitch P, Karlawish JH,

Rowe CC, Carillo MC, Hartley DM, Hedrick S, Pappas V, Thies W; Alzheimer's Association; Society of Nuclear Medicine and Molecular Imaging; Amyloid Imaging Taskforce. Appropriate use criteria for amyloid PET: a report of the Amyloid Imaging Task Force, the Society of Nuclear Medicine and Molecular Imaging, and the Alzheimer's Association. Dual publication in: Alzheimer's Dement 2013; 9: e-1-16. J Nucl Med 2013; 54: 476-490.

[2] Klunk WE, Engler H, Nordberg A, Wang Y, Blomqvist G, Holt DP, Bergström M, Savitcheva I, Huang GF, Estrada S, Ausén B, Debnath ML, Barletta J, Price JC, Sandell J, Lopresti BJ, Wall A, Koivisto P, Antoni G, Mathis CA, Långström B. Imaging brain amyloid in Alzheimer's disease with Pittsburgh Compound-B. Ann Neurol 2004; 55: 306-319.

[3] Rowe CC, Ackerman U, Browne W, Mulligan R, Pike KL, O'Keefe G, Tochon-Danguy H, Chan G, Berlangieri SU, Jones G, Dickinson-Rowe KL, Kung HP, Zhang W, Kung MP, Skovronsky D, Dyrks T, Holl G, Krause S, Friebe M, Lehman L, Lindemann S, Dinkelborg LM, Masters CL and Villemagne VL. Imaging of amyloid beta in Alzheimer's disease with ^{18}F-BAY94-9172, a novel PET tracer: proof of mechanism. Lancet Neurol 2008; 7: 129-135.

[4] Nelissen N, Van Laere K, Thurfjell L, Owenius R, Vandenbulcke M, Koole M, Bormans G, Brooks DJ and Vandenberghe R. Phase 1 study of the Pittsburgh compound B derivative ^{18}F-flutemetamol in healthy volunteers and patients with probable Alzheimer disease. J Nucl Med 2009; 50: 1251-1259.

[5] Wong DF, Rosenberg PB, Zhou Y, Kumar A, Raymont V, Ravert HT, Dannals RF, Nandi A, Brasić JR, Ye W, Hilton J, Lyketsos C, Kung HF, Joshi AD, Skovronsky DM and Pontecorvo MJ. In vivo imaging of amyloid deposition in Alzheimer disease using the radioligand ^{18}F-AV-45 (florbetapir ^{18}F). J Nucl Med 2010; 51: 913-920.

[6] Fleisher AS, Chen K, Liu X, Roontiva A, Thiyyagura P, Ayutyanont N, Joshi AD, Clark CM, Mintun MA, Pontecorvo MJ, Doraiswamy PM, Johnson KA, Skovronsky DM and Reiman EM. Using positron emission tomography and florbetapir ^{18}F to image cortical amyloid in patients with mild cognitive impairment or dementia due to Alzheimer disease. Arch Neurol 2011; 68: 1404-1411.

[7] Joshi AD, Pontecorvo MJ, Clark CM, Carpenter AP, Jennings DL, Sadowsky CH, Adler LP, Kovnat KD, Seibyl JP, Arora A, Saha K, Burns JD, Lowrey MJ, Mintun MA and Skovronsky DM. Performance characteristics of amyloid PET with florbetapir ^{18}F in patients with alzheimer's disease and cognitively normal subjects. J Nucl Med 2012; 53: 378-384.

[8] Joshi, AD, Pontecorvo MJ, Lu M, Skovronsky DM, Mintun MA and Devous MD. A semi-automated method for quantification of florbetapir ^{18}F PET images. J Nucl Med 2015; 56: 1736-1741.

[9] Johnson KA, Sperling RA, Gidicsin CM, Carmasin JS, Maye JE, Coleman RE, Reiman EM, Sabbagh MN, Sadowsky CH, Fleisher AS, Murali Doraiswamy P, Carpenter AP, Clark CM, Joshi AD, Lu M, Grundman M, Mintun MA and Pontecorvo MJ. Florbetapir (^{18}F-AV-45) PET to assess amyloid burden in Alzheimer's disease dementia, mild cognitive impairment, and normal aging. Alzheimers Dement 2013; 9: S72-S83.

[10] Doraiswamy PM, Sperling RA, Johnson K, Reiman EM, Wong TZ, Sabbagh MN, Sadowsky CH, Fleisher AS, Carpenter A, Joshi AD, Lu M, Grundman M, Mintun MA, Skovronsky DM and Pontecorvo MJ. Florbetapir ^{18}F amyloid PET and longitudinal cognitive decline: A prospective 36-month multicenter study. Mol Psychiatry 2014; 19: 1044-51.

[11] Tateno A, Sakayori T, Higuchi M, Suhara T, Ishihara K, Kumita S, Suzuki H and Okubo Y. Amyloid imaging with [^{18}F] florbetapir in geriatric depression: early-onset versus late-onset. Int J Geriatr Psychiatry 2015; 30: 720-728.

[12] Kawas CH, Greenia DE, Bullain SS, Clark CM, Pontecorvo MJ, Joshi AD and Corrada MM. Amyloid imaging and cognitive decline in nondemented oldest-old: The 90+ Study. Alzheimer Dis Assoc Disord 2013; 9: 199-203.

[13] Landau SM, Breault C, Joshi AD, Pontecorvo MJ, Mathis CA, Jagust WJ and Mintun MA. Amyloid-β imaging with Pittsburgh compound B and florbetapir: comparing radiotracers and quantification methods. J Nucl Med 2013; 54: 70-77.

[14] Clark CM, Schneider JA, Bedell BJ, Beach TG, Bilker WB, Mintun MA, Pontecorvo MJ, Hefti F, Carpenter AP, Flitter ML, Krautkramer MJ, Kung HF, Coleman RE, Doraiswamy PM, Fleisher AS, Sabbagh MN, Sadowsky CH, Reiman EP, Zehntner SP and Skovronsky DM. Use of florbetapir-PET for imaging beta-amyloid pathology. JAMA 2011; 305: 275-283.

[15] Clark CM, Pontecorvo MJ, Beach TG, Bedell BJ, Coleman RE, Doraiswamy PM, Fleisher AS, Reiman EM, Sabbagh MN, Sadowsky CH, Schneider JA, Arora A, Carpenter AP, Flitter ML, Joshi AD, Krautkramer MJ, Lu M, Mintun MA and Skovronsky DM. Cerebral PET with florbetapir compared with neuropathology at autopsy for detection of neuritic amyloid-beta plaques: a prospective cohort study. Lancet Neurol 2012; 11: 669-678.

[16] Friston KJ, Ashburner JT, Kiebel SJ, Nichols TE and Penny WD. Statistical parametric map-

ping: the analysis of functional brain images. In: Friston KJ, Ashburner JT, Kiebel SJ, Nichols TE and Penny WD, editors. London, U.K.: Academic Press; 2007.

[17] Evans A, Collins, DL, Mills SR, Brown ED, Kelly RL and Peters TM. 3D statistical neuroanatomical models from 305 MRI volumes. IEEE Nucl Sci Symp Med Imag Conf 1993; 1813-1817.

[18] International Atomic Energy Agency, Quantitative Nuclear Medicine Imaging: Concepts, Requirements and Methods, IAEA Human Health Reports No. 9. Vienna: IAEA; 2014.

[19] Avril N, Bense S, Ziegler SI, Dose J, Weber W, Laubenbacher C, Römer W, Jänicke F, Schwaiger M. Breast imaging with ^{18}F-FDG PET: quantitative image analysis. J Nucl Med 1997; 38: 1186-91.

[20] Lin C, Itti E, Haioun C, Petegnief Y, Luciani A, Dupuis J, Paone G, Talbot JN, Rahmouni A and Meignan M. Early ^{18}F-FDG PET for prediction of prognosis in patients with diffuse large B-cell lymphoma: SUV-based assessment versus visual analysis. J Nucl Med 2007; 48: 1626-32.

[21] Foster NL Heidebrink JL, Clark CM, Jagust WJ, Arnold SE, Barbas NR, DeCarli CS, Turner RS, Koeppe RA, Higdon R and Minoshima S. FDG-PET improves accuracy in distinguishing frontotemporal dementia and Alzheimer's disease. Brain 2007; 130: 2616-2635.

[22] Piper JW. Quantitative comparison of spatial normalization algorithms for 3D PET brain scans. J Nucl Med 2007; 48: S403.

[23] Cook RD and Weisberg S. Residuals and influence in regression. New York, New York: Chapman and Hall; 1982.

[24] Bollen KA and Jackman RW. Regression diagnostics: An expository treatment of outliers and influential cases. Modern methods of data analysis. In: Fox F, Long JS, editors. Newbury Park, CA: Sage; 1990. pp. 257-291.

[25] Klunk WE, Koeppe RA, Price JC, Benzinger TL, Devous MD Sr, Jagust WJ, Johnson KA, Mathis CA, Minhas D, Pontecorvo MJ, Rowe CC, Skovronsky DM and Mintun MA. The Centiloid Project: Standardizing quantitative amyloid plaque estimation by PET. Alzheimers Dement 2015; 11: 1-15, e1-4.

[26] Camus V, Payoux P, Barré L, Desgranges B, Voisin T, Tauber C, La Joie R, Tafani M, Hommet C, Chételat G, Mondon K, de La Sayette V, Cottier JP, Beaufils E, Ribeiro MJ, Gissot V, Vierron E, Vercouillie J, Vellas B, Eustache F and Guilloteau D. Using PET with ^{18}F-AV-45 (florbetapir) to quantify brain amyloid load in a clinical environment. Eur J Nucl Med Mol Imaging 2012; 39: 621-31.

[27] Guerra UP, Nobili FM, Padovani A, Perani D, Pupi A, Sorbi S and Trabucchi M. Recommendations from the Italian Interdisciplinary Working Group (AIMN, AIP, SINDEM) for the utilization of amyloid imaging in clinical practice. Neurol Sci 2015; 36: 1075-1081.

[28] Kobylecki C, Langheinrich T, Hinz R, Vardy E, Brown G, Martino M, Haense C, Richardson A, Gerhard A, Anton-Rodriguez J, Snowden J, Neary D, Pontecorvo M and Herholz K. [^{18}F]-florbetapir positron emission tomography in patients with frontotemporal dementia and Alzheimer's disease. J Nucl Med 2015; 56: 386-391.

[29] Perani D, Schillaci O, Padovani A, Nobili FM, Iaccarino L, Della Rosa PA, Frisoni G, Caltagirone C. A survey of FDG and amyloid-PET imaging in dementia and GRADE analysis. Biomed Res Int 2014; 2014: 785039.

[30] Thal DR, Beach TG, Zanette M, Heurling K, Chakrabarty A, Ismail A, Smith AP and Buckley C. [^{18}F]flutemetamol amyloid positron emission tomography in preclinical and symptomatic Alzheimer's disease: Specific detection of advanced phases of amyloid-β pathology. Alzheimers Dement 2015; 11: 975-985.

[31] Villemagne VL, Burnham S, Bourgeat P, Brown B, Ellis KA, Salvado O, Szoeke C, Macaulay SL, Martins R, Maruff P, Ames D, Rowe CC and Masters CL. Amyloid β deposition, neurodegeneration and cognitive decline in sporadic Alzheimer's disease: a prospective cohort study. Lancet Neurol 2013; 12: 357-67.